Supporting Information (SI)

Re-Examining the Size/Charge Paradigm: Differing *In Vivo* Characteristics of Size and Charge-Matched Mesoporous Silica Nanoparticles

Jason L. Townson[1,‡], Yu-Shen Lin[1,‡], Jacob O. Agola[1], Eric C. Carnes[3], Hon S. Leong[5], John D. Lewis[6], Christy L. Haynes[7], and C. Jeffrey Brinker[1,2,4,]*

[1]Center for Micro-Engineered Materials, [2]Department of Chemical and Nuclear Engineering, the University of New Mexico, Albuquerque, New Mexico 87131, United States, [3]Nanobiology Department, [4]Self-Assembled Materials Department, Sandia National Laboratories, Albuquerque, New Mexico 87185, United States, [5]London Regional Cancer Program, London, Canada, [6]Department of Oncology, University of Alberta, Edmonton, Canada, [7]Department of Chemistry, University of Minnesota, Minneapolis, Minnesota, 55455, USA

[⊥]These authors contributed equally.

* To whom correspondence should be addressed.

E-mail: cjbrink@sandia.gov, Web: http://www.unm.edu/~solgel/

1. Experimental details

1.1 Chemicals and reagents. All chemicals and reagents were used as received. Acetic anhydride, 3-aminopropyltriethoxysilane (98%, APTES), ammonium nitrate (NH_4NO_3), n-cetyltrimethylammonium bromide (CTAB), N,N-dimethyl formamide (DMF), dimethyl sulfoxide (DMSO), rhodamine B isothiocynate (RITC), and tetraethyl orthosilicate (TEOS) were purchased from Sigma-Aldrich (St. Louis, MO). Ammonium hydroxide (NH_4OH, 28-30%) was obtained from VWR (West Chester, PA). Hydrochloric acid (36.5-38%, HCl), and pyridine were purchased from EMD Chemicals (Gibbstown, NJ). Absolute ethanol was obtained from Pharco-Aaper (Brookfield, CT). Trimethoxysilylpropyl modified polyethyleneimine (50% in isopropanol, MW 1500-1800, PEI-silane), *N*-trimethoxysilylpropyl-*N*,*N*,*N*-trimethyl ammonium chloride (50% in methanol, TMAC-silane), and 2-[methoxy(polyethyleneoxy)propyl]trimethoxysilane (MW 550-750, 9-12 EO, PEG-silane) were purchased from Gelest Inc. (Morrisville, PA). Fetal bovine serum (FBS), 10X phosphate buffered silane (PBS) and penicillin streptomycin (PS) were purchased from Gibco (Logan, UT). Dulbecco's Modification of Eagle's Medium with 4.5 g/L glucose, L-glutamine and sodium pyruvate (DMEM) was obtained from CORNING cellgro (Manassas, VA).

1.2 Mesoporous silica nanoparticle (MSNP) synthesis. Synthesis of stable RITC-incorporated PEG/PEI and PEG/NMe_3^+ MSNPs (designated as PEG-PEI and PEG-NMe_3^+): To prepare RITC-labeled PEG/PEI MSNPs, 3 mg of RITC was first dissolved in 2 mL of DMF and 1.5 µL of APTES was then added and the stirred at room temperature for 4 h to prepare the RITC-APTES solution. Then, 150 mL of 5.3 mM CTAB ammonium hydroxide solution was prepared in a 250 mL beaker, sealed with parafilm, and placed in an oil bath at 50 ^oC. After continuously stirring for 1 h, 2.5 mL of dilute TEOS solution (prepared in ethanol) was added to the surfactant solution. After another hour stirring, 450 µL of PEG-silane and 20 µL of PEI-silane were added consecutively to the MS colloidal solution under stirring. Thirty minutes later, stirring was stopped and the as-synthesized RITC-PEG/PEI colloidal solution was aged at 50 ^oC for 10 h. After aging, the obtained particle solution (~50 mL) underwent a

hydrothermal treatment reported by Haynes and co-workers.[1] The further NP purification procedure followed a previously reported method.[2] For $PEG_{650/5k}$-PEI particles, 0.1 g of PEG_{5k} (Creative PEGWorks, Winston Salem, NC) was added immediately following addition of short chain PEG (225 µL) as above. All other synthesis conditions were the same. For RITC-labeled PEG-NMe^{3+} MSNP synthesis, the only difference was using TMAC-silane (250 µL) instead of PEI-silane. For large 150-nm-diameter PEG-NMe_3^+ MSNP synthesis, the concentration of NH_4OH and the amount of TMAC-silane were changed 0.512 M of NH_4OH and 300 µL of TMAC-silane, respectively. Otherwise, the synthesis procedure was similar to 50 nm PEG-PEI and PEG-NMe_3^+ MSNPs.

Acetylation of PEG/PEI MSNPs: For acetylation of PEG/PEI MSNPs, 2 mg of PEG/PEI MSNPs was dispersed to 1 mL of DMF by centrifugation. Then, 20 µL of acetic anhydride and 10 µL of pyridine were added to the PEG/PEI NP solution. After 30 min, the acetylated particles were centrifuged and redispersed in 1 mL of DMF. The acetylation reaction on the particles was repeated one time. The acetylated particles were washed with D.I. water 3 times by centrifugation. Finally, the acetylated PEG-PEI MSNPs were dispersed in DI water at 2 mg/mL.

1.4 Material Characterization. Nitrogen adsorption-desorption isotherms: The sorption isotherms of RITC-labeled PEG-PEI and PEG-NMe^{3+} MSNPs were obtained from on a Micromeritics ASAP 2020 (Norcross, GA) at 77 K. Samples were degassed at 120 ^oC for 12 h before measurements. The surface area and pore size was calculated from the Brunauer-Emmet-Teller (BET) equation and standard Barrett-Joyer-Halenda (BJH) method. Hydrodynamic size and zeta potential measurements: The hydrodynamic size and zeta potential of MSNPs were measured on a Malvern Zetasizer Nano-ZS equipped with a He-Ne laser (633 nm) and Non-Invasive Backscatter optics (NIBS). The samples for dynamic light scattering (DLS) measurements were suspended in various media (DI, PBS, DMEM, and DMEM+10% FBS) at 1 mg/mL. All the hydrodynamic size and zeta potential measurements were carried out at 25 ^oC. DLS measurements for each sample were obtained at least three runs. The hydrodynamic size of all samples was reported using a z-average diameter. For zeta potential data, each

sample was measured at least 100 runs. All the reported values correspond to the average of at least three independent samples.

1.5 Cell culture. A-431 (ATCC CRL-1555) human adenocarcinoma, A549 (ATCC CCL-185) human lung carcinoma, Hep3B (ATCC HB-8064) human hepatocellular carcinoma, and human hepatocyte (ATCC CRL-11233) cells from American Type Culture Collection (Manassas, VA) were maintained in high glucose Dulbecco's Modified Eagle Medium (DMEM) (CORNING Cellgro, VA) containing 10% fetal bovine serum (FBS) at 37°C and 5% CO_2.

1.6 Flow cytometry. To study the binding difference of PEG-PEI, PEG-NMe_3^+, and PEG-PEI-ace MSNPs to various types of cells, $5x10^5$ suspension cells (A549, A431, Hep3B, or hepatocytes) were incubated with 10 μg/mL of NPs at 37 ^{0}C under 5% CO_2 for 30 min. After NP exposure, cells were washed with PBS twice and then fixed in 1 mL of 3.7% formaldehyde PBS solution for 15 min). After fixation, cells were further washed with PBS one time before flow cytometry measurements. All flow cytometry based measurements were performed in 1x PBS, pH 7.4 buffer (Gibco Life Technologies, Grand Island, NY). Becton-Dickinson FACScalibur flow cytometer (Sunnyvale, CA) interfaced to a Power PC Macintosh using the CellQuest software package was used. The instrument is equipped with a 15 mW air-cooled argon ion laser, emitting at 488 nm. The signal detection system of the cytometer uses five detectors: a) high performance solid state silicon detector with 488-nm band pass filter for forward scatter detection; b) high performance photomultiplier using Brewster angle beam splitter in the emission optical train for side scatter detection and c) four photomultiplier tubes for fluorescence detection at fixed wavelengths of 530, 585, 670 and 661-nm (FL1, FL2, FL3 and FL4 respectively). Fixed band pass filters are used for wavelength selection and are optimized for the desired emission. For measurements on the flow cytometer, mammalian cell samples were transferred to a tube suitable (Product No. 352008, BD Bioscience, San Jose, CA) for flow cytometry and were diluted at least 10-fold in 1x PBS. The dilution step was not only necessary to ensure discrimination between cell-

associated fluorescence and background fluorescence arising from unbound NPs, but also ensured that sufficient sample volume for the measurement was used. The required fluorescence signal was detected and recorded on the FL2 channel. Raw data obtained from the flow cytometer were processed using FlowJo software (Tree Star, Inc. Ashland, OR).

1.7 Cell viability assay. Water-soluble tetrazolium salt (WST-8) assay: The cell viability of A431 and A549 after NP incubation was determined using a cell counting kit-8 (CCK-8, Dojindo, Rockville, MD). First, 6 x 10^4 cells were seeded in a 96-well plate and cultured in DMEM+10%FBS at 37 ^oC under 5% CO_2 for 24 h. Then the cells were incubated with 100 µL of different concentrations of NP solutions. After 24h incubation, the NP-treated cells were washed with serum-free DMEM two times. After washing, 10 µL of CCK-8 solution was added to each well containing 100 µL of serum-free DMEM. After another 1h incubation at 37 ^oC (5% CO_2), the absorbance of the mixture medium was measured at 450 nm using a BioTek microplate reader. The viability was calculated using the following equation.

$$Viability\ from\ WST-8\ assay\ (\%) = \left(\frac{sample\ abs_{450nm}}{control\ abs_{450nm}}\right) \times 100$$

Lactate dehydrogenase (LDH) assay: The cell membrane integrity of A549 and A431 cells after NP exposure was assessed by a commonly used LDH assay. The procedure of NP exposure to cells was the same as described in the previous WST-8 assay section. The LDH activity in the cell culture medium was measured using a BioVision LDH cytotoxicity assay kit (Milpitas, CA). The percent LDH release from NP treated cells was calculated using the following equation. Cells without NP exposure and lysed cell (by surfactant addition) were used as the negative and positive control, respectively.

$$Percent\ LDH\ Release\ (\%) = \left(\frac{sample\ abs_{455nm} - negative\ control\ abs_{455nm}}{positive\ control\ abs_{455nm} - negative\ control\ abs_{455nm}}\right) \times 100$$

1.9 Hemolysis assay. Human whole blood (sodium EDTA stabilized) was purchased from Innovative Research (Novi, MI). The washed human red blood cells (hRBCs) were obtained by following a published procedure.[1] The washed hRBCs were exposed to PEG-PEI and PEG-NMe_3^+ MSNPs at different concentrations. All the samples were placed on a rocking shaker in an incubator at 37 ^{0}C for 2 h. D.I. water (+hRBCs) and PBS (+hRBCs) were used as the positive control and negative control, respectively. Then the absorbance of hemoglobin in the supernatant was measured by a BioTek microplate reader (Winooski, VT) at 541 nm. The hemolysis percentage of each NP treated sample was determined using the following equation.

$$Percent\ hemolysis\ (\%) = \left(\frac{sample\ abs_{541nm} - negative\ control\ abs_{541nm}}{positive\ control\ abs_{541nm} - negative\ control\ abs_{541nm}}\right) \times 100$$

1.8 *Ex ovo* avian embryos. The *ex ovo* chick embryo procedure followed has been described previously[3] and was conducted following institutional approval (Protocol 11-100652-T-HSC). Briefly, eggs were acquired from East Mountain Hatchery (Edgewood, NM) and placed in a GQF 1500 Digital Professional incubator (Savannah, GA) for 3-4 days. Embryos were then removed from shells by cracking into 100ml polystyrene weigh boats (VWR). *Ex ovo* embryos were covered and returned to incubator with constant humidity (~70%) and temperature (~39 ^{o}C). 50 µg (at 1 mg/ml) of NPs in PBS were injected into secondary or tertiary veins via pulled glass capillary needles. Embryo chorioallantoic membrane (CAM) vasculature was imaged using a customized avian embryo chamber and a Zeiss AxioExaminer upright microscope with heated stage.

Table S1. Total surface area and pore size of PEG-PEI and PEG-NMe_3^+ MSNPs

Sample	BET surface area (m^2/g)	BJH pore size (nm)
PEG-PEI	507	2.3
PEG-NMe_3^+	473	2.1

Figure S1

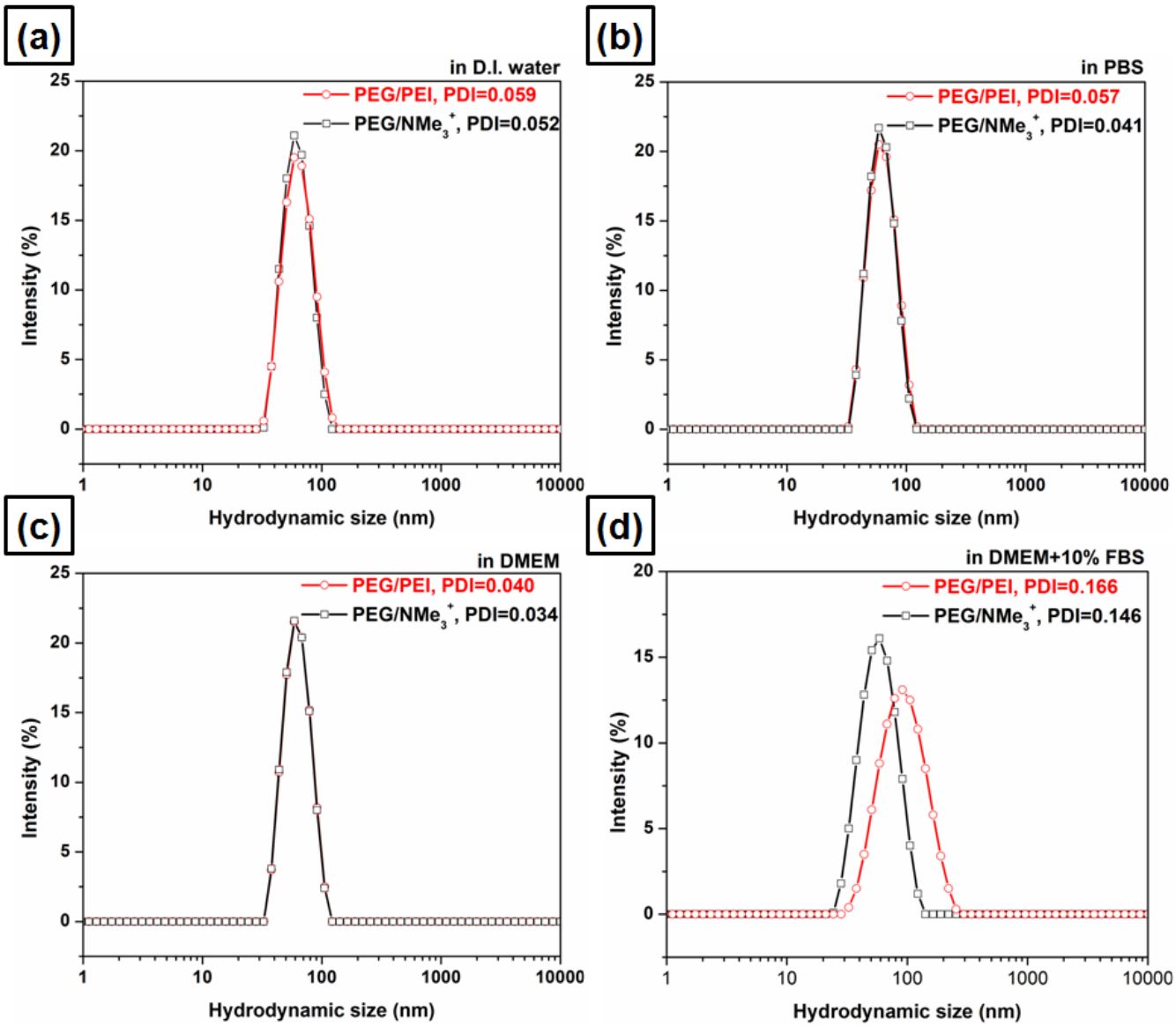

Figure S1. Representative hydrodynamic size distribution of PEG-PEI, PEG-NMe_3^+, and PEG-PEI-ace MSNPs (1 mg/mL) measured at RT in various solutions: (a) D.I. water, (b) PBS, (c) DMEM, and (d) DMEM+10% FBS.

Figure S2

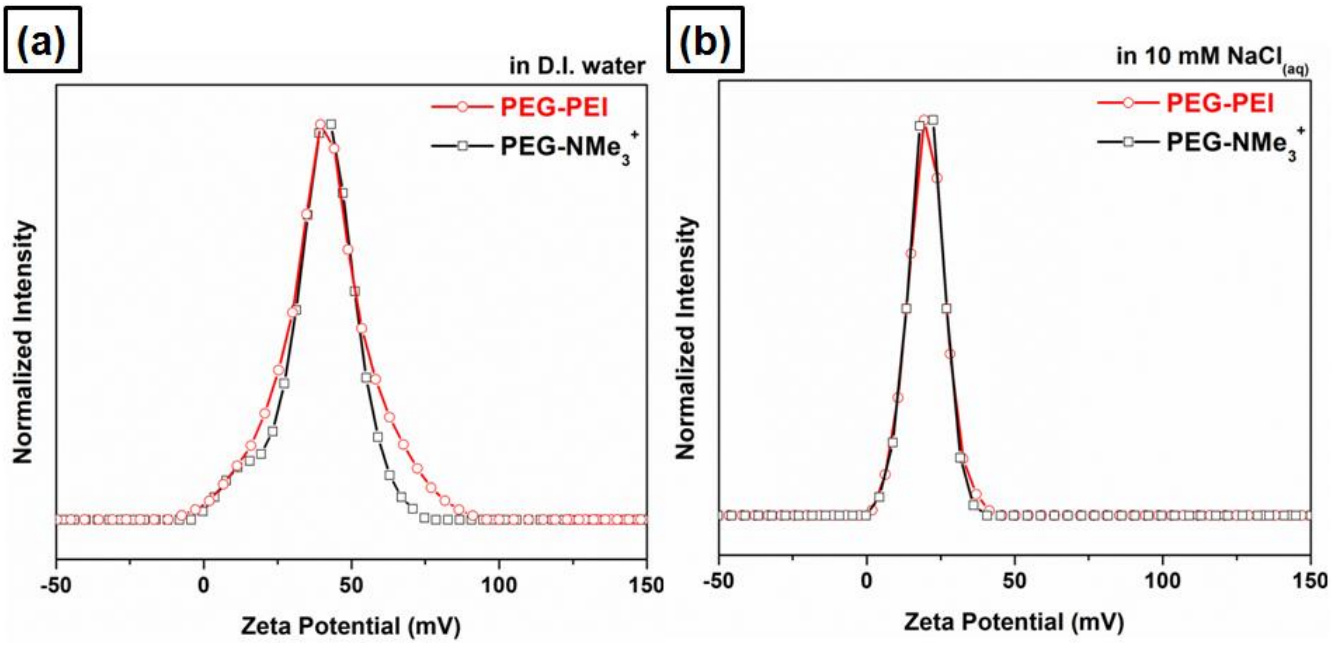

Figure S2. Surface charge distribution of PEG/PEI and PEG/NMe_3^+ MSNPs in (a) D.I. water and (b) 10 mM $NaCl_{(aq)}$.

Figure S3

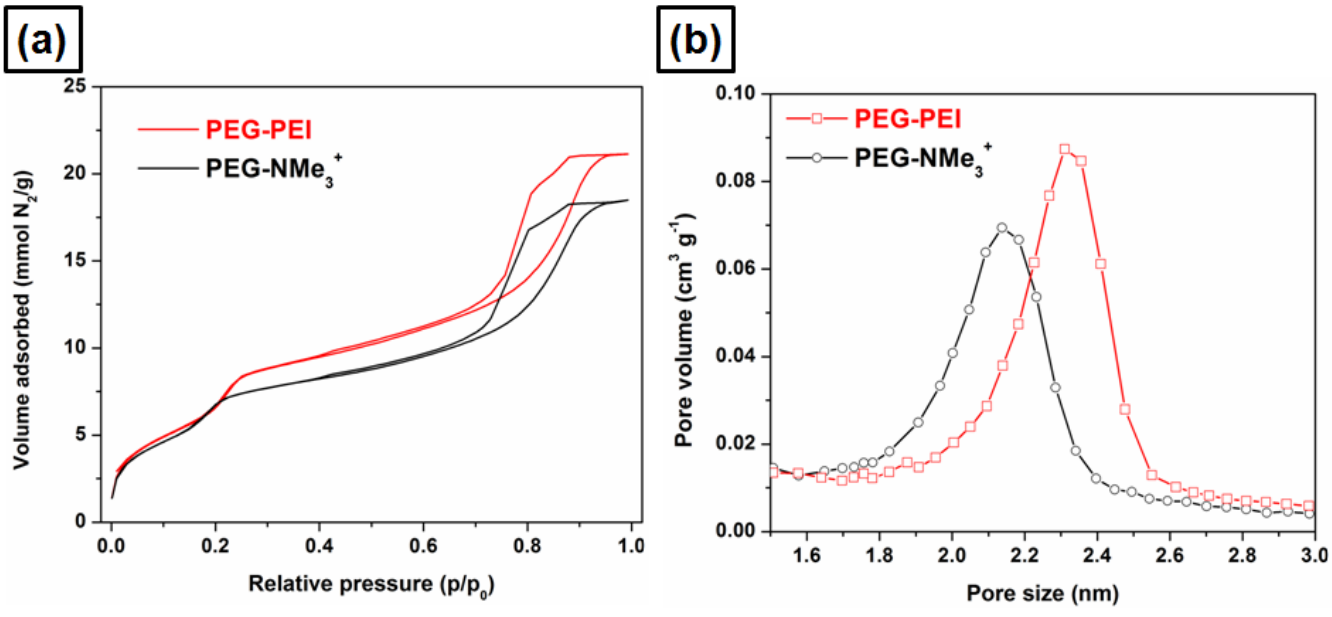

Figure S3. (a) N_2 adsorption-desorption isotherms and (b) BJH pore size distribution of PEG-PEI and PEG-NMe_3^+ MSNPs.

Figure S4

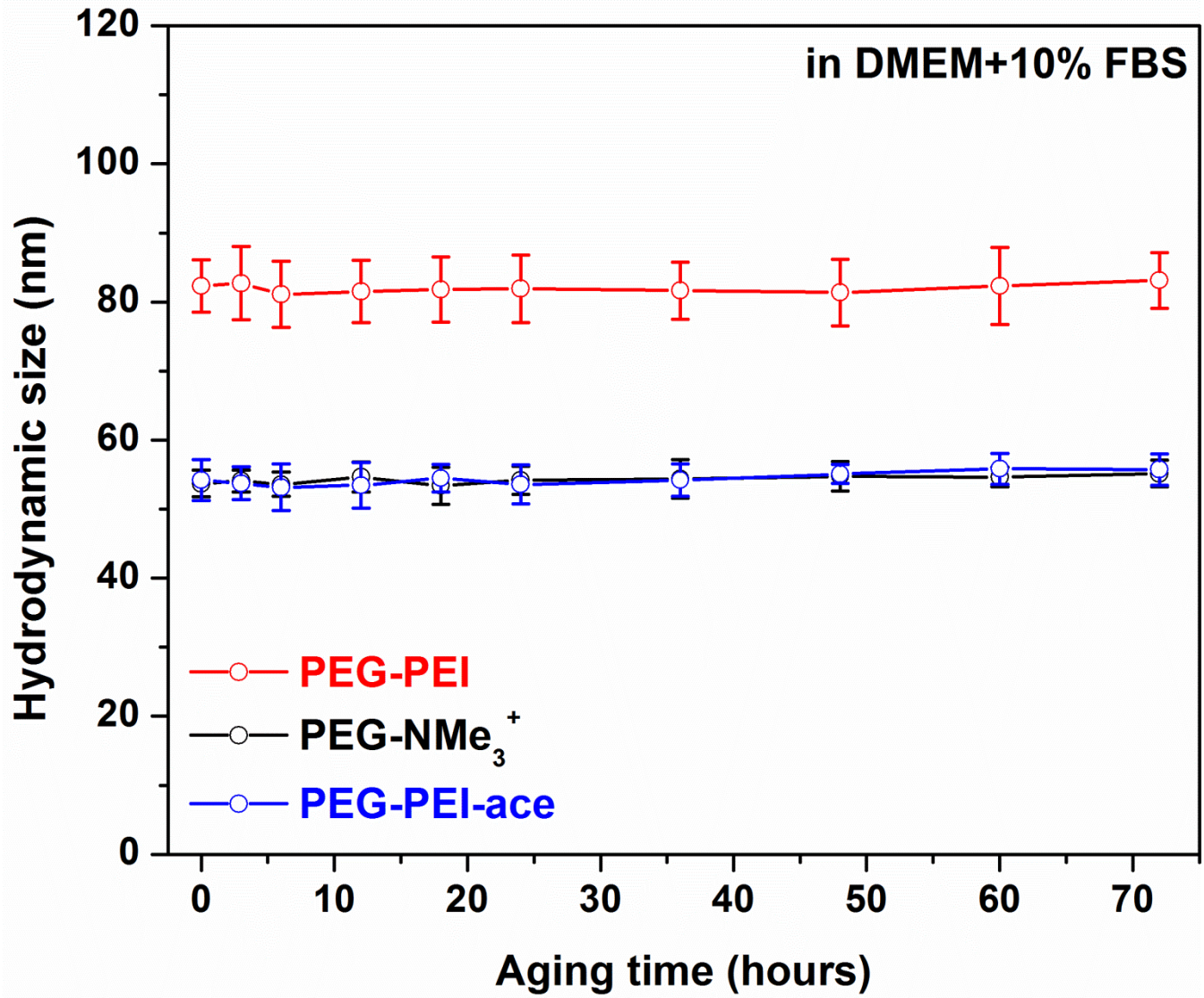

Figure S4. Long term particle stability of PEG-PEI, PEG-NMe_3^+, and PEG-PEI-ace MSNPs.

Figure S5

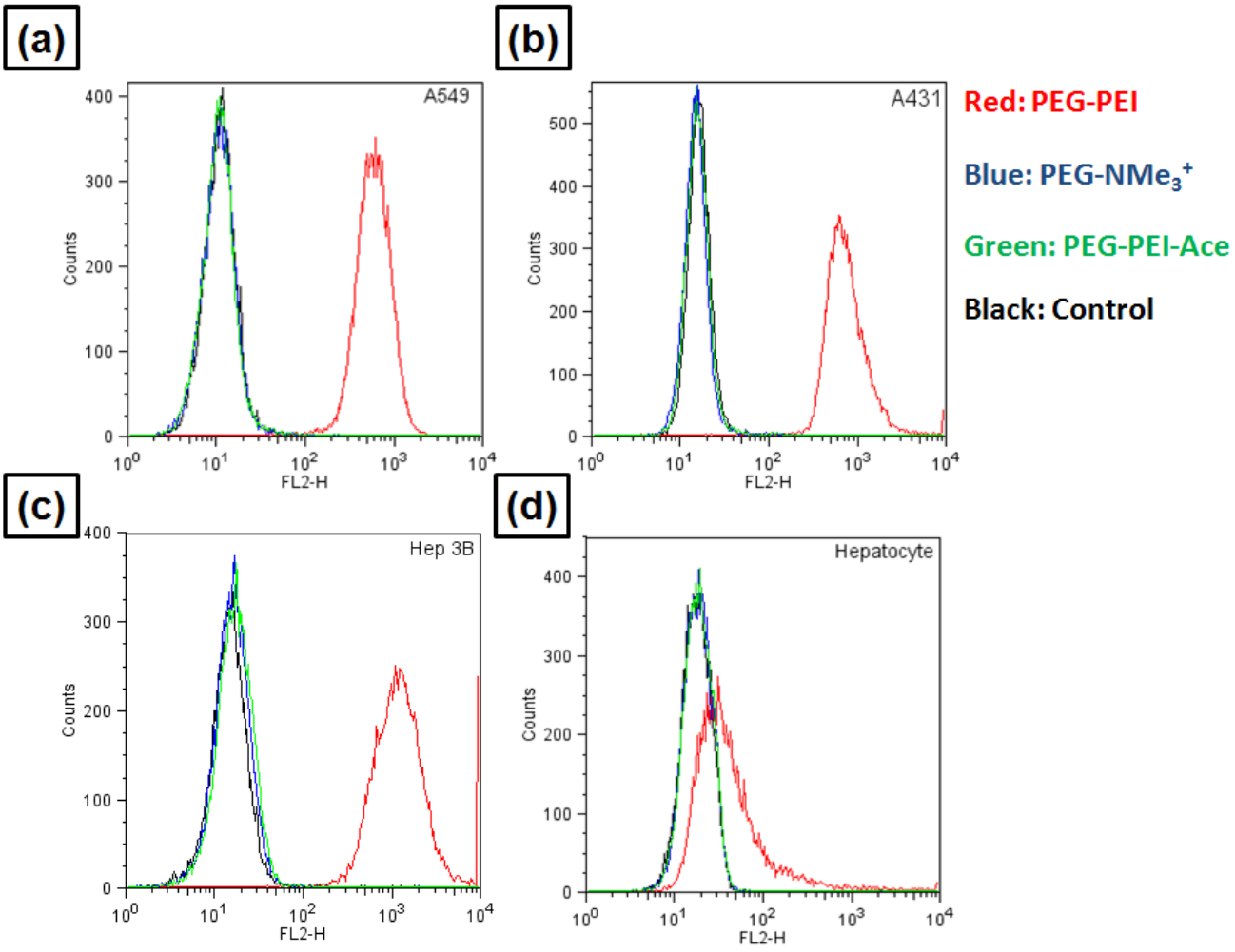

Figure S5. Flow cytometry of (a) A549, (b) A431, (c) Hep3B, and (d) hepatocyte cells after 30 min incubation with 10 µg/mL PEG-PEI, PEG-NMe_3^+ or PEG-PEI-ace MSNPs at 37 ^oC under 5% CO_2. Flow data was generated in the Flow Cytometry Shared Resource Center supported by the University of New Mexico Health Sciences Center and the University of New Mexico Cancer Center.

Figure S6

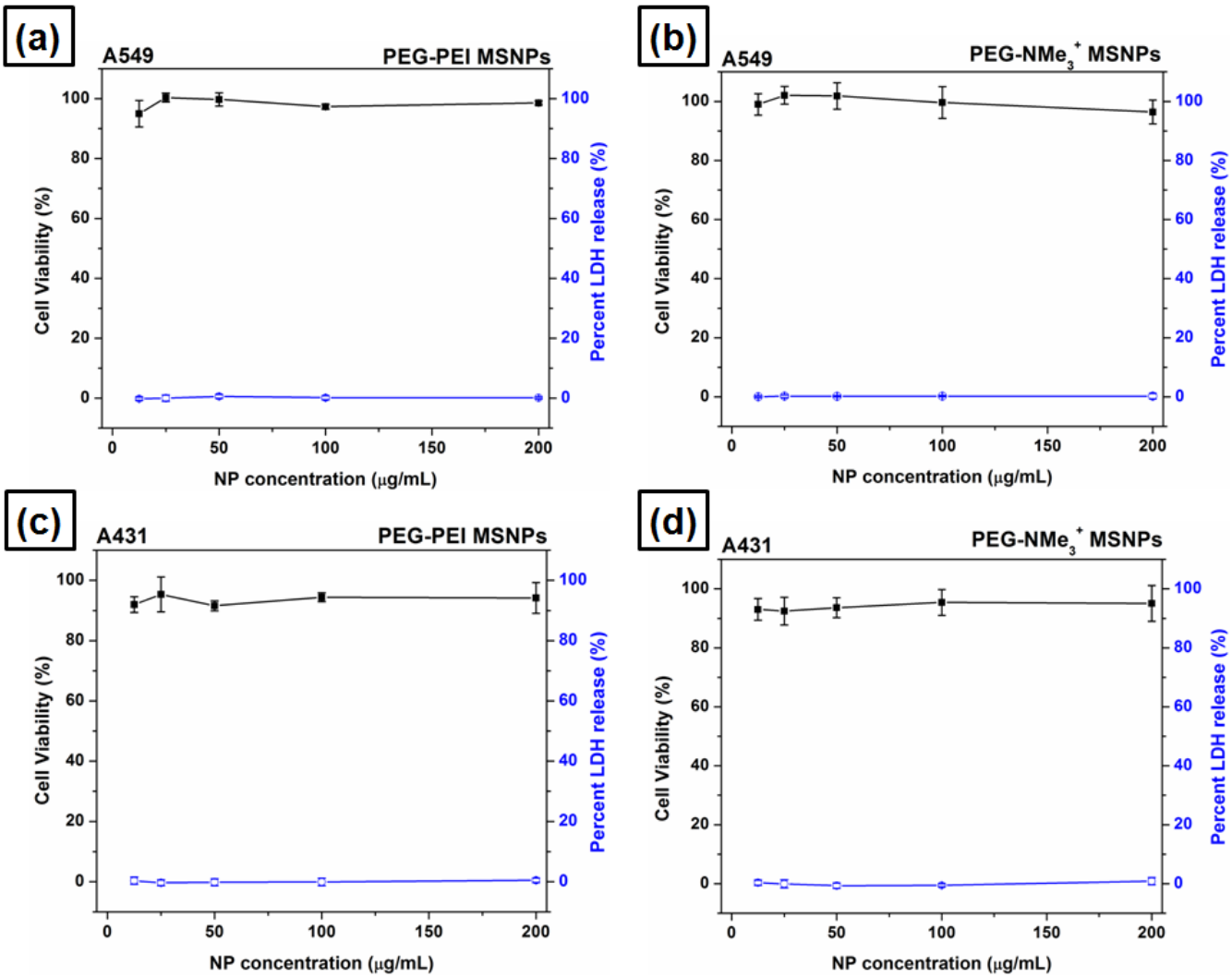

Figure S6. Cell viability of A549 (a,b) and A431 (c,d) cells determined from WST-8 and LDH assay after 24 h exposure to various concentrations (12.5, 25, 50, 100, and 200 μg/mL) of PEG-PEI and PEG-NMe_3^+ MSNPs. Data represent mean ± SD (n=4).

Figure S7

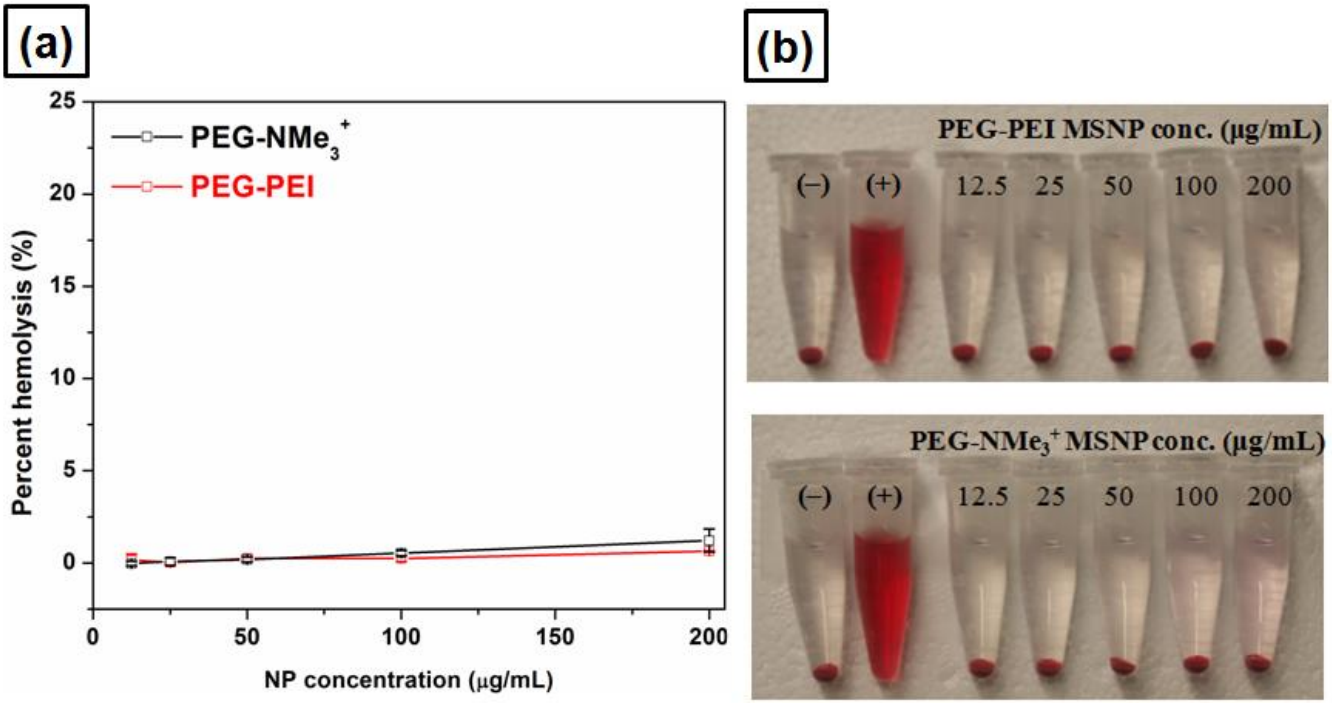

Figure S7. (a) Percentage of lysed human red blood cells (hRBCs) after exposure to 12.5, 25, 50, 100, and 200 μg/mL) of PEG-PEI and PEG-NMe_3^+ MSNPs for 2 h at 37 ^oC. Data represent mean ± SD (n=3). (b) Digital photographs of hRBCs after 2 h incubation to PEG-PEI and PEG-NMe_3^+ MSNPs at different concentrations (12.5 to 200 μg/mL). The presence of red hemoglobin in the supernatant indicates membrane damaged hRBCs. The (+) and (-) symbols represent positive control and negative control, respectively.

Figure S8

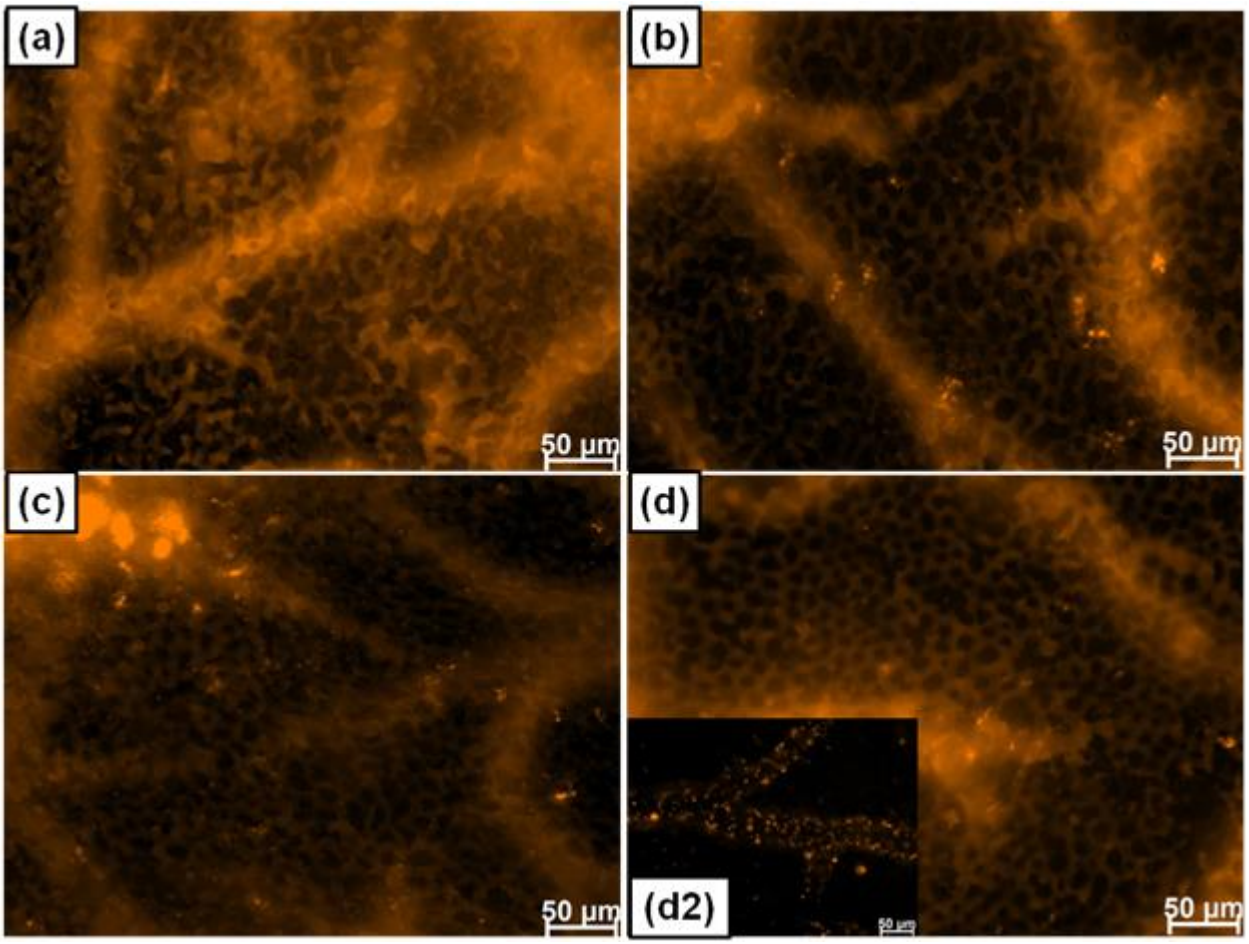

Figure S8. Vascular circulation of PEG-NMe_3^+ and PEG-PEI-Ace particles over time. (a-c) PEG-NMe_3^+ MSNPs (a) immediately, (b) 1 h and (c) 6 h post injection. Note in all cases particles are primarily circulating and vasculature with little binding to endothelium observed. (d) PEG-PEI-Ace MSNPs (3 h post injection) continue to circulate with no apparent endothelium binding observed. (d2) 21 h post injection PEG-PEI-Ace particle binding is observed in large venules differing from immediate capillary binding observed with unmodified PEG-PEI particles.

Figure S9

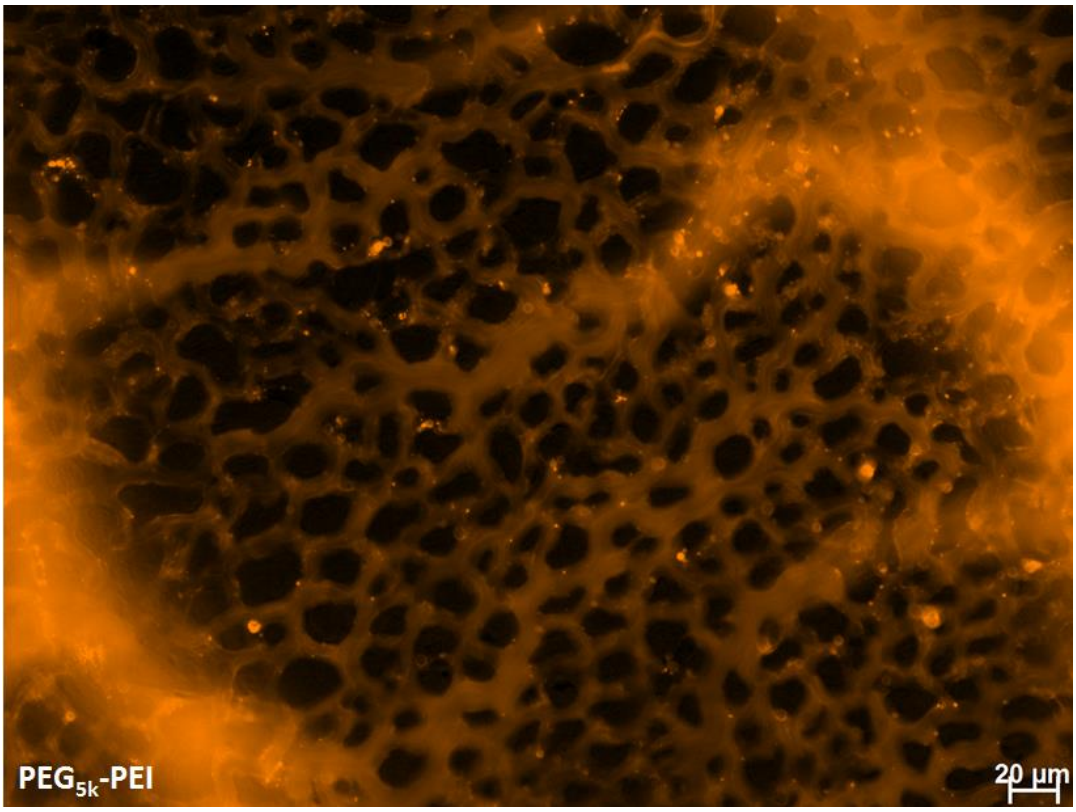

Figure S9. $PEG_{650/5k}$-PEI particles synthesized to include a longer chain PEG (MW 5000) exhibited decreased binding (relative to short PEG-PEI particles) to CAM capillary endothelium and WBCs immediately after injection. Reduced binding is likely due to a decrease in PEI accessibility. $PEG_{650/5k}$-PEI particles false colored orange.

Figure S10

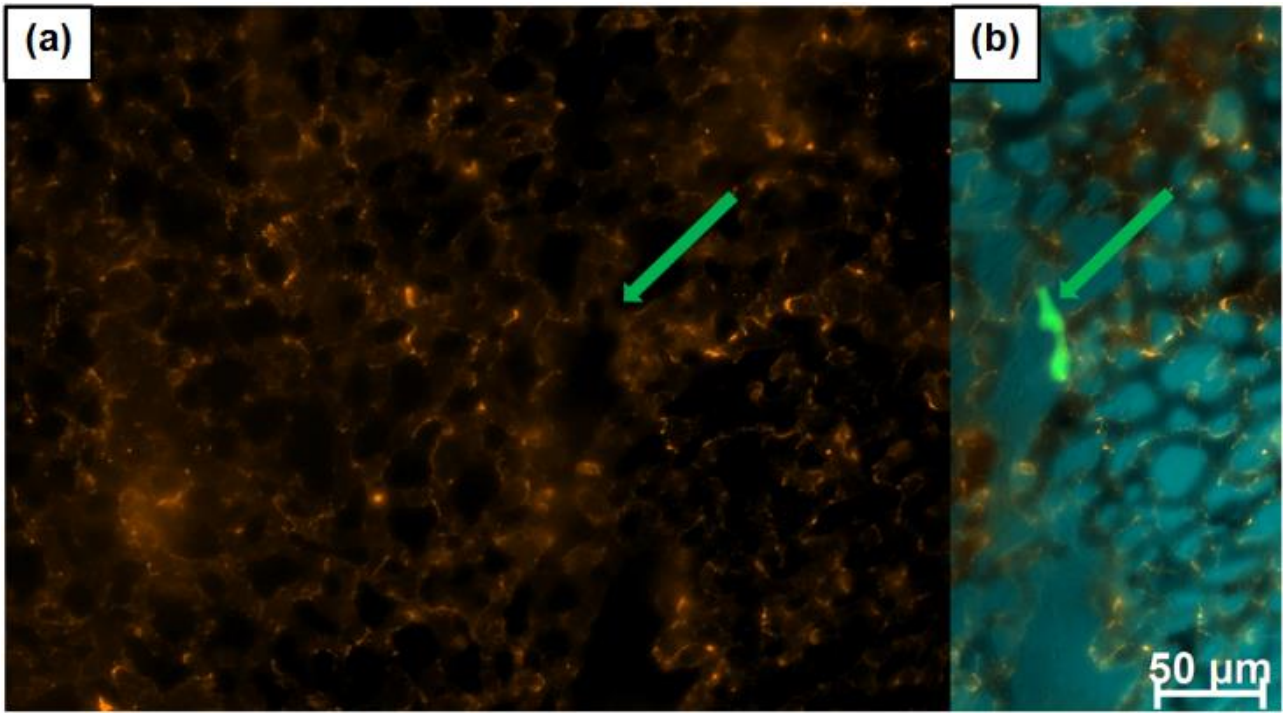

Figure S10. PEG-PEI MSNPs deposit on the vessel walls and are scavenged by white blood cells of CAM immediately following injection, with no apparent binding to cancer cells. (a) Particles binding to vasculature and WBCs with no specific out-line of a cancer cell (location indicated by arrow). (b) Merged particle and cancer cells (green) image. CAM tissue autofluorescence is false colored blue.

Figure S11

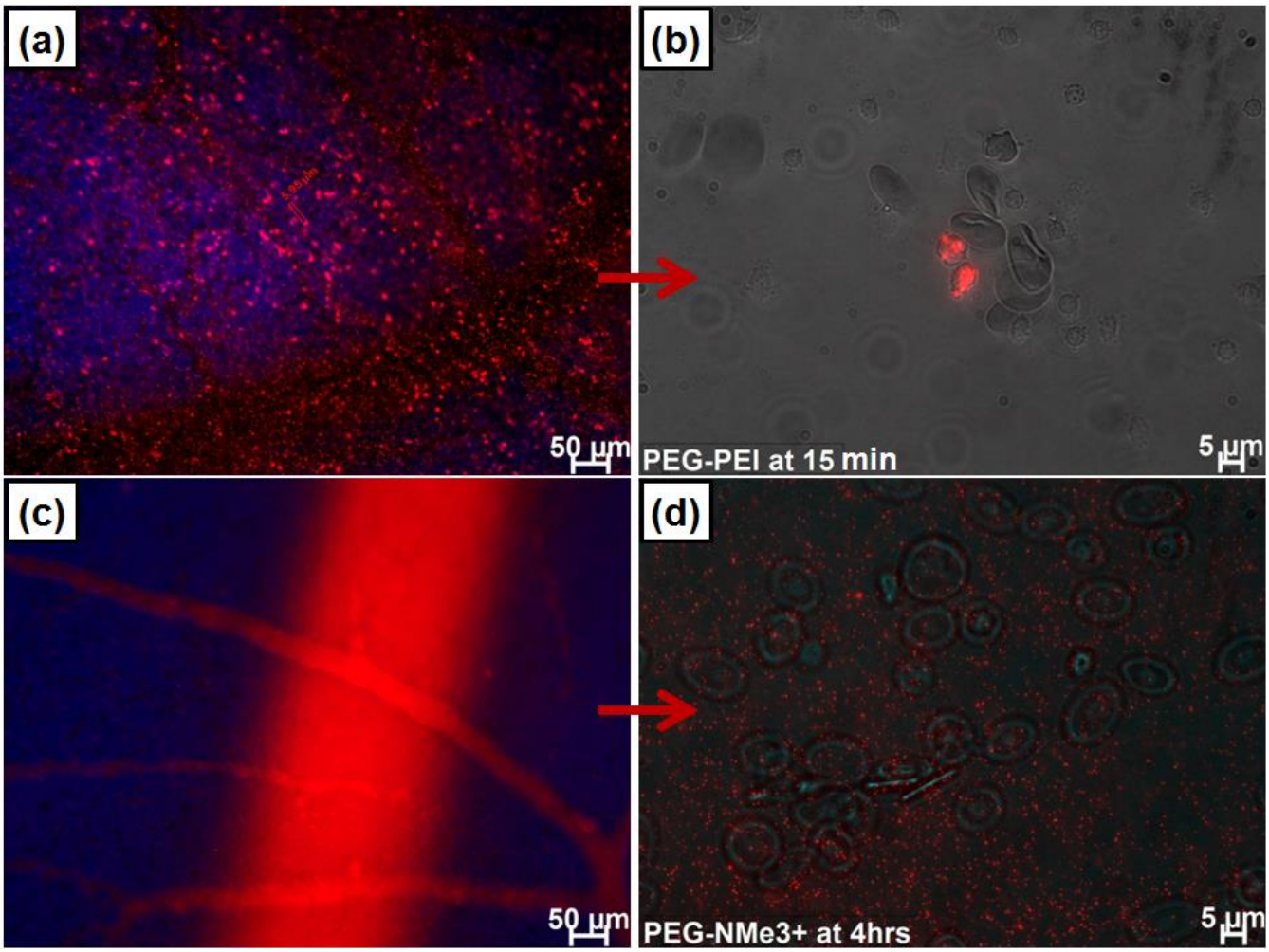

Figure S11. *In vivo* and *ex vivo* red and white blood cell-NP interactions. (a) PEG-PEI MSNP binding immediately post injection in CAM. Particles are observed lining the endothelium as well as adhered to 6-8 µm sized cells but not red blood cells. (b) Blood samples removed 15 min post injection of PEG-PEI MSNPs. Few particles observed in solution with most apparent adhered to white blood cells (red spots) but not red blood cells. (c) PEG-NMe_3^+ particles 3 h post injection. (d) Whole blood removed 4 h post injection of PEG-NMe_3^+ NPs. Particles are visible in blood with no apparent binding to white or red blood cells.

Figure S12

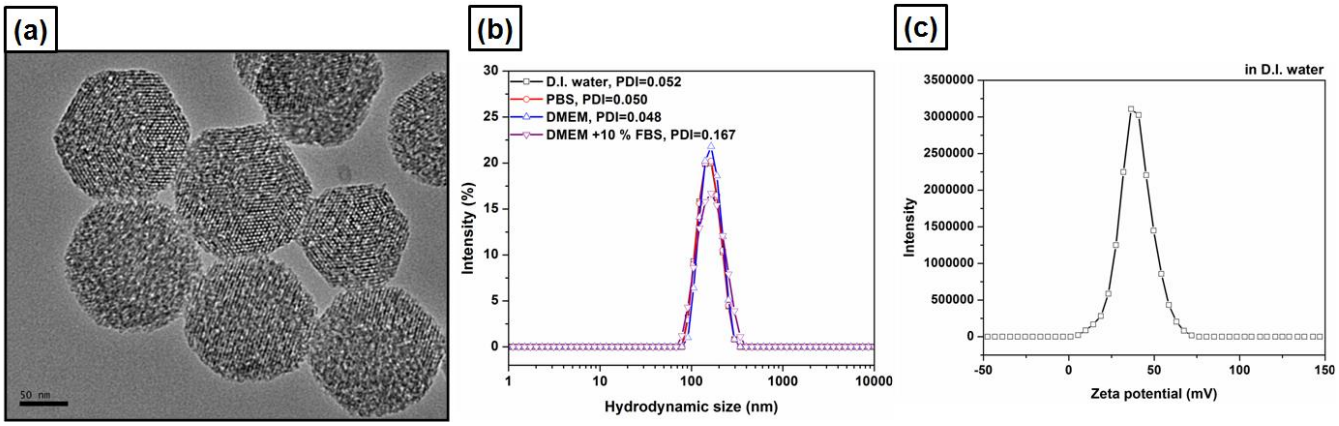

Figure S12. (a) TEM image of 150 nm PEG-NMe_3^+ MSNPs. (b) Representative hydrodynamic size distribution of 150 nm PEG-NMe_3^+ MSNPs (1 mg/mL) measured at RT in various solutions: D.I. water, PBS, DMEM, and DMEM+10% FBS. (c) Zeta potential distribution of 150 nm PEG-NMe_3^+ MSNPs measured in D.I. water.

Table S2. Hydrodynamic size and surface charge of 150 nm PEG-PEI MSNPs

D_h in DI water (nm)	D_h in PBS (nm)	D_h in DMEM (nm)	D_h in DMEM+10% FBS (nm)	ζ in DI water(mV)	ζ in 10 mM $NaCl_{(aq)}$(mV)
158.3 ± 11.2	159.5 ± 12.9	156.3 ± 13.7	148.9 ± 10.1	+39.7 ± 3.6	+19.4 ± 1.8

Video S1. Representative video of blood flow patterns in chick CAM. CAM stroma is apparent as bright spots due to autofluorescence while red blood cells are observed circulating within arteries, veins and the capillary bed. Arteries and veins are apparent below the capillary bed as larger dark vessels.

Video S2. Video of chick CAM immediately post injection of 50 nm PEG-PEI particles. Endothelial and WBC binding is apparent at this early time point. Moving spherical clusters are PEG-PEI particles

bound to WBCs in circulation. Smaller punctuate fluorescence is due to particles bound to endothelial cells.

Video S3. Video of chick CAM immediately post injection of 150 nm PEG-NMe_3^+ particles. Particles continue to circulate in the vasculature with minimal binding to endothelium or WBCs observed.

References:

1. Lin, Y.-S.; Abadeer, N.; Hurley, K. R.; Haynes, C. L. *J. Am. Chem. Soc.* **2011**, *133*, 20444-20457.

2. Lin, Y.-S. Abadeer, N.; Haynes, C. L. *Chem. Comm.* **2011**, *47*, 532-534.

3. Leong, H.S.; Steinmetz, N. F.; Ablack A.; Destito, G.; Zijlstra, A.; Stuhlmann, H.; Manchester, M; Lewis, J. D. *Nat Protoc*. **2010**, *5*, 1406-1417.